Tamura, Y., Busby, C.J., Blum, P., and the Expedition 350 Scientists
Proceedings of the International Ocean Discovery Program Volume 350
publications.iodp.org

doi:10.14379/iodp.proc.350.201.2016

Data report: Pleistocene planktonic foraminiferal oxygen and carbon stable isotope records and their use to improve the age model of Hole U1436C cores recovered east of the Aogashima Volcano[1]

Maryline J. Vautravers[2] and the Expedition 350 Scientists[3]

Keywords: International Ocean Discovery Program, IODP, *JOIDES Resolution*, Expedition 350, Site U1436, Hole U1436C, stable isotope stratigraphy, Pleistocene, planktonic foraminifers

Contents

Abstract

International Ocean Discovery Program (IODP) Expedition 350 cored Site U1436 at intermediate water depth (1776 meters below sea level) in the western part of the Izu fore-arc basin, ~60 km east of the arc-front volcano, Aogashima. Site U1436 lies 1.5 km west of Ocean Drilling Program Site 792 (Leg 126). Site U1436 (proposed Site IBM-4), conceived as a 150 m deep geotechnical test hole for future deep drilling (5500 meters below seafloor) with the D/V *Chikyu,* provides a rich record of Pleistocene volcanism. Isotopic stratigraphy data reported here extend the timescale and improve the precision of the shipboard-determined biostratigraphy to enhance further investigations on the nature, origin, and rhythm of the volcanic eruptions recorded at this site.

The $\delta^{18}O$ and $\delta^{13}C$ values in selected samples containing planktonic foraminifers (*Neogloboquadrina dutertrei*) were measured over the 70 m long record from Hole U1436C. Isotopic ratios were determined for 167 samples and are examined in conjunction with nannofossil and planktonic foraminifer datums obtained during Expedition 350. These data allow fairly good identification of all marine isotope stages over the last 1 My. The results from this data report provide a refined age scale that will enhance the scientific appeal of this site to volcanologists and sedimentologists and increase the potential impact of their interpretations in later research stages. Hole U1436C was cored near the Kuroshio Current in the North Pacific Ocean realm, where any new paleoceanographic and paleoclimatologic data would be valuable. Furthermore, the refined stratigraphic framework from this study also clearly shows that the original goals of Expedition 350 can easily be expanded beyond that of the study of the evolution of the Earth's crust toward new targets focused on Earth surface processes.

Introduction

During International Ocean Discovery Program (IODP) Expedition 350 on board the R/V *JOIDES Resolution*, two sites were cored at intermediate water depth in the western Pacific Ocean (Philippine Sea). The main focus of the expedition was IODP Site U1437, at which rear-arc evolution over the last 10 My will be studied using the sedimentary record of changing volcanism through time recovered from an interval extending to 1800 meters below seafloor (mbsf). In contrast, IODP Site U1436 was initially thought of as an ancillary target because it was intended as a short (150 m) geotechnical hole to prepare for potential future drilling at proposed Site IBM-4 using the D/V *Chikyu*, which has the capacity to drill to the arc middle crust target at 5500 mbsf. Nonetheless, Site U1436 yielded a potentially continuous record of Late Pleistocene fore-arc sediments influenced by arc-front explosive volcanism. This site, therefore, provides an opportunity to investigate in a rather proximal location (i.e., near the volcanic island of Aogashima) (Figure **F1**) the detailed history and evolution of Late Pleistocene volcanism within the Izu arc. This additional goal became particularly appealing once drilling had to be stopped at Site U1437 and a contingency plan was put in place. Indeed, this change meant that Site U1436 could be cored through more than one hole to improve the quality of the entire section (i.e., with fewer intervals lost to coring disturbance) as well as more particularly in an interval containing a conspicuously thick black glassy mafic ash layer. The preliminary age for this layer, based on the age model constructed for Hole U1436A, was estimated to be about 0.75 Ma. Core recovery at Site U1436 was excellent, particularly in Hole U1436C, with 100% recovery for the 70 m cored. The samples used in this study were taken exclusively from Hole U1436C because of the limited time available for sam-

[1] Vautravers, M.J., and the Expedition 350 Scientists, 2016. Data report: Pleistocene planktonic foraminiferal oxygen and carbon stable isotope records and their use to improve the age model of Hole U1436C cores recovered east of the Aogashima Volcano. *In* Tamura, Y., Busby, C.J., Blum, P., and the Expedition 350 Scientists, *Izu-Bonin-Mariana Rear Arc*. Proceedings of the International Ocean Discovery Program, 350: College Station, TX (International Ocean Discovery Program). http://dx.doi.org/10.14379/iodp.proc.350.201.2016
[2] Godwin Laboratory for Paleoclimate research, Earth Sciences Department, University of Cambridge, Downing Street, Cambridge CB2 3EQ, United Kingdom. **mv217@cam.ac.uk**
[3] **Expedition 350 Scientists' addresses.**
MS 350-201: Received 3 June 2015 · Accepted 5 April 2016 · Published 6 July 2016

Figure F1. Location of Expedition 350 Hole U1436C and Ocean Drilling Program (ODP) Leg 126 Sites 792, 786, and 787. Site U1436 lies 60 km east of Aogashima, an arc-front mafic volcano that forms a small and inhabited island. Figure was slightly modified from the **Expedition 350 summary** chapter (Tamura et al., 2015b).

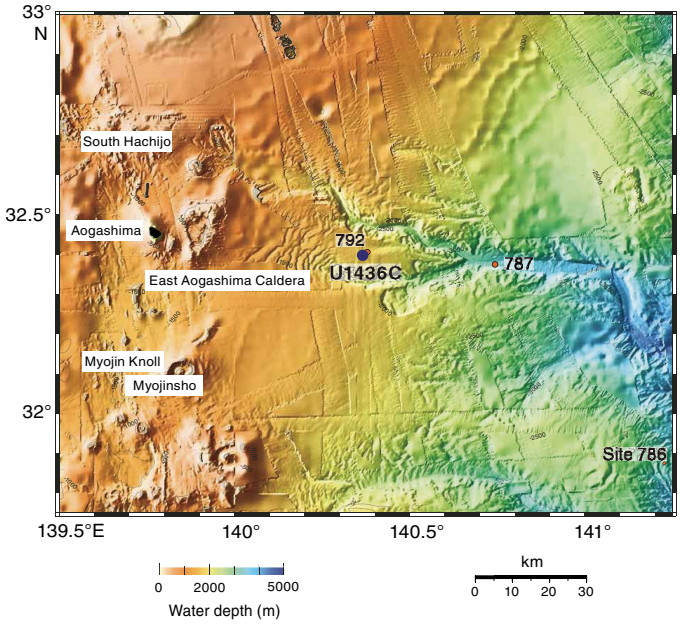

pling, which was conducted after Expedition 350 during the transit at the start of IODP Expedition 351, because of the absence of a composite section, and because Hole U1436C was mostly cored using the half-length advanced piston corer (HLAPC) and is consequently much less disturbed than cores from Hole U1436A.

A quick assessment of the samples prior to picking revealed low abundances and discontinuous downcore occurrences of benthic foraminiferal species commonly used for stable isotope studies (e.g., *Cibicides* or *Uvigerina*). Therefore, one planktonic foraminifer species was chosen instead. At such a subtropical site (~32°N; Figure **F1**) and in the vicinity of the Kuroshio Current, the thermocline-dwelling species *Neogloboquadrina dutertrei* (see inset image in Figure **F2** for illustration) has the best likelihood to be both well preserved and abundant enough in one single, narrow size fraction throughout the whole section to be able to provide a continuous isotope record for the site over the Upper Pleistocene.

It is well established that oxygen isotopes in marine calcite, in particular in foraminifer tests, provide an excellent record of glacial–interglacial cycles. They capture the water $\delta^{18}O$ composition through a composite recording of the effects of local water temperature changes (Emiliani, 1955) and global changes in ocean $\delta^{18}O$ composition, which varies through time as a consequence of changing ice volume (Shackleton, 1967). Within the limitation imposed by the need for continuous recording (i.e., no missing cycles), the regular and cyclic pattern shown by $\delta^{18}O$ and its global nature makes it now a classic (i.e., used routinely for ~50 y) and straightforward tool

Figure F2. Hole U1436C downcore depth plots of oxygen ($\delta^{18}O$) and carbon ($\delta^{13}C$) isotope ratios on the planktonic foraminifer *Neogloboquadrina dutertrei* (inset: specimen from Sample 350-U1437B-1H-CC, blue scale bar = 300 µm) (data in Table **T1**). Changes in isotopic ratios are in per mil versus Vienna Peedee belemnite (VPDB). Horizontal red line = conspicuous black glassy mafic ash layer.

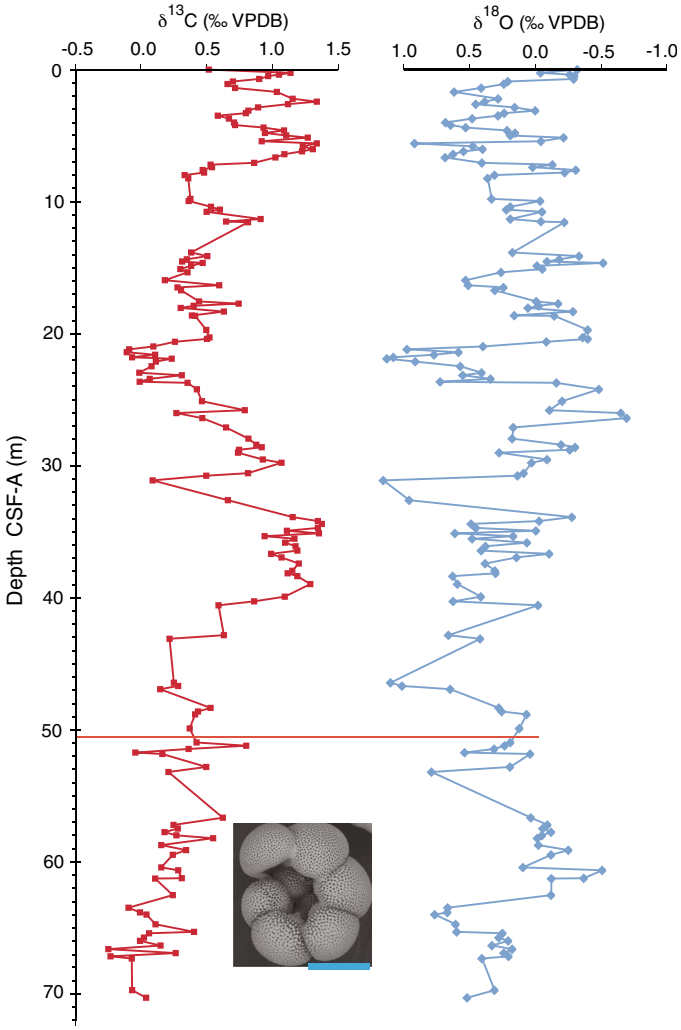

for stratigraphic correlation and nonabsolute dating. This is particularly true for the Neogene (i.e., the last 23.5 My) (Gradstein et al., 2012), over which $\delta^{18}O$ provides a highly accurate record. We visually correlated our oxygen isotope record from Hole U1436C to a stacked $\delta^{18}O$ benthic record, the so-called LR04 (Figure **F3B**), which has a resolution of ~1 ky and was developed from the compilation of the benthic $\delta^{18}O$ data from 57 marine sites by Lisiecki and Raymo (2005). This allowed us to transfer our newly obtained stable isotope record from its depth scale to an age scale and establish a more detailed and precise stratigraphy than that obtained via biostratigraphy only (see the **Expedition 350 methods** chapter [Tamura et al., 2015a]).

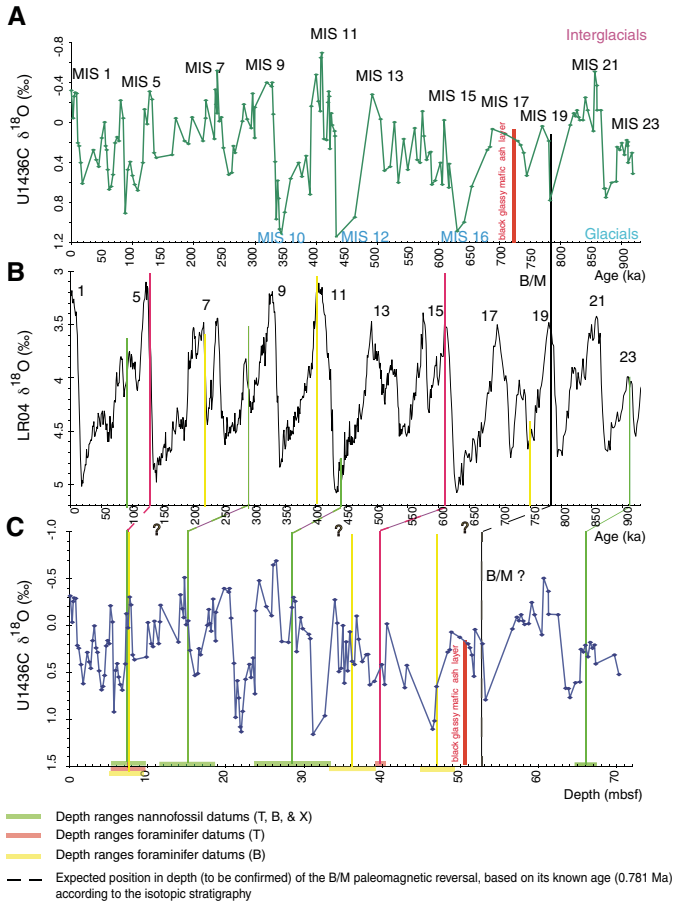

Figure F3. A. Oxygen isotope variations vs. age in Hole U1436C rescaled using AnalySeries 2.0.4.2 software and tie points in Table **T2**. Paleoclimatic stratigraphy with glacials = even MIS numbers, interglacials = odd MIS numbers. Vertical red line = stratigraphic position of major black mafic ash layer. B. Benthic $\delta^{18}O$ reference curve (LR04 stack; Lisiecki and Raymo, 2005) with numbered interglacial stages. C. Oxygen isotope variations vs. depth from 0 to 70 mbsf, Hole U1436C. Colored vertical lines = average depths of nannofossil and planktonic foraminifer datums. Expected position of Brunhes/Matuyama (B/M) paleomagnetic reversal was deduced from observations in Hole U1436A. All datums are from Expedition 350 (see the **Site U1436** chapter [Tamura et al., 2015c]) and are presented in Table **T3**.

Material and methods

Samples

The material cored in Hole U1436C consists mainly of unconsolidated tuffaceous mud and mud with ash as well as numerous distinct ash or lapilli layers of suspected varied geochemical compositions and volcanic sources (see the **Site U1436** chapter [Tamura et al., 2015c]). Routine shipboard core catcher biostratigraphy samples were collected at regular intervals set by the core length without regard for lithology. To increase the chances of obtaining higher biogenic content (i.e., yielding foraminifers) necessary for the analyses, additional samples for this study were collected exclusively from layers of tuffaceous mud and mud with ash recognized on the basis of core description and images; ash and lapilli layers were carefully avoided. This strategy was important to produce a record from one single species in one standardized size fraction along the entire record. This is known to yield better results. Altogether, a total of 212 samples taken from the 70 m long Hole U1436C section were used. Of these, 194 samples were selected for the present study, whereas 18 are the designated shipboard "micropaleontological samples." These last samples are systematically/routinely taken during paleoceanographic expeditions on the *JOIDES Resolution* at the base of each core (i.e., in each core catcher) in order to establish the preliminary biostratigraphic scale for each site (see the **Site U1436** chapter [Tamura et al., 2015c]).

In the sediment preparation laboratory, each of the 194 purpose-selected sediment samples of ~10 cm^3 was placed in a flask containing deionized water (~100 cm^3) and disaggregated on a shaking table for a few hours prior to sieving on a 63 µm sieve. After drying, this technique yields the required coarse fraction (>63 µm). Following a well-established procedure of the Godwin Laboratory (e.g., Vautravers et al., 2013), all size fractions are kept so the concentrations (number of particles per gram of dry bulk sediment) can be calculated and the fine fractions can be used later for additional analyses. The 18 core catcher samples were prepared following a method used on board the *JOIDES Resolution* (see the **Site U1436** chapter [Tamura et al., 2015c]). This last method, being less time consuming, is more suitable for shipboard work, but the fine fractions are not kept, so it does not allow for quantitative estimates at any stage. Although highly variable between samples, the coarse fractions (>63 µm) consist mostly of planktonic foraminifer shells and their fragments, but they usually also contain abundant ash and other volcanic particles of various colors and sizes. Accessory biogenic silica content, mostly radiolarians, is observed in most samples but in variable abundances. Similarly, benthic foraminifers are found in all samples but are usually rare. A systematic and detailed analysis of the micropaleontological samples has been carried out. It is noticeable that the foraminiferal content in each of the >150 µm size fractions (a size fraction commonly used elsewhere in micropaleontological studies; e.g., Vautravers et al., 2004) ranges from rare to abundant (Vautravers et al., submitted), in agreement with shipboard observations (see the **Expedition 350 methods** chapter [Tamura et al., 2015a]). For example, in a few samples selected across a range of contrasted interglacials and glacials, the abundances were 1109 foraminifers/g during the Holocene or marine isotope Stage (MIS) 1 (Sample 350-U1436C-1H-1, 0–2 cm; 0 mbsf), 119 foraminifers/g during MIS 11 (Sample 6H-2, 110–112 cm; 26.4 mbsf), 3646 foraminifers/g during MIS 23 (Sample 17F-2, 40–42 cm; 66.6 mbsf), and 3694 foraminifers/g during MIS 10 (Sample 5H-2, 66–68 cm; 20.96 mbsf). Paleoceanographic implications of the changing planktonic foraminifer concentrations are presented and discussed in Vautravers et al. (submitted).

In the micropaleontological laboratory, a few to about 30 unbroken and clean *N. dutertrei* specimens (sized between 250 and 300 µm) were selected from each sample for isotopic analysis, whenever possible. Using a fine brush and distilled water, careful selection of clean specimens without any dark specks (i.e., oxides) or mud infilling is particularly important because the analytical method (Gasbench) used for the stable isotope analyses does not involve any further cleaning step, as is usual (i.e., a short and light 3% H_2O_2 treatment) of the foraminiferal calcite. The absence of the cleaning step arises from the type of vial used on Gasbench, which does not allow it. The exact number of shells per sample to be analyzed was recorded, and each sample was weighed to check that they were either larger than or close to 100 mg. *N. dutertrei* shell weights are also reported in Vautravers et al. (submitted).

Isotopic analyses

Our immediate analytical goal was to pick enough tests of *N. dutertrei* for as many samples as possible to have at least 100 µg of calcite available for analyses of the $\delta^{18}O$ and $\delta^{13}C$ ratios downcore. This was possible for 167 of the 221 samples that were selected outside the numerous ash and lapilli layers in order to increase the chances of planktonic foraminifer tests recovery (i.e., avoid extreme dilution by volcaniclastic sediments). Nonetheless, 45 samples did not yield enough *N. dutertrei* specimens. This was primarily a result of intense calcium carbonate dissolution, despite the relatively shallow water depth (1776 m), coupled with strong dilution by lithogenic particles in some cases.

Each sample of ~100 to >300 µm of dried foraminiferal calcite (see above) was transferred into a tall Exetainer vial (12 mL) and sealed with a silicone rubber septa using a screw cap. The samples were flushed with CP (5.0) grade helium, acidified with orthophosphoric acid, and left to react for 1 h at 70°C. The samples were analyzed using a Thermo Gasbench preparation system attached to a Thermo MAT-253 mass spectrometer in continuous flow mode. Each sample batch (30 samples each) was accompanied by 10 reference carbonate samples (Carrara Z) and 2 control samples (Fleton Clay). Carrara Z has been calibrated to the Vienna Peedee belemnite (VPDB) standard using the international standard NBS-19. Measurement precision is better than ±0.08‰ for $\delta^{13}C$ and ±0.10‰ for $\delta^{18}O$. As a standard procedure for planktonic foraminifer samples, which are made of pluri-specimens (at least about 10), no replicates were run in this study. All isotopic results, calibrated against VPDB, are presented versus depth in Table **T1** and are plotted versus depth (Figures **F2**, **F3C**) and versus age (Figure **F3A**) according to the isotopic stratigraphy suggested here on the basis on the tie points presented in Table **T2**.

Table T1. Values of oxygen isotope ratios and stable carbon isotope ratios, Hole U1436C. (Continued on next page.) **Download table in .csv format.**

Core, section, interval (cm)	Top depth CSF-A (m)	$\delta^{18}O$ (‰ VPDB)	$\delta^{13}C$ (‰ VPDB)
350-U1436C-			
1H-1, 0–2	0	–0.32	0.51
1H-1, 25–27	0.25	–0.04	1.14
1H-1, 38–40	0.38	–0.26	1.05
1H-1, 50–52	0.5	–0.30	0.97
1H-1, 70–72	0.7	–0.29	0.90
1H-1, 90–92	0.9	0.21	0.70
1H-1, 110–112	1.1	0.24	0.66
1H-1, 138–140	1.38	0.41	0.71
1H-2, 18–20	1.68	0.62	1.03
1H-2, 70–72	2.2	0.28	1.15
1H-2, 92–94	2.42	0.38	1.34
1H-2, 112–114	2.62	0.45	1.12
1H-2, 136–138	2.86	0.16	0.89
1H-3, 10–12	3.1	–0.00	0.82
1H-3, 30–32	3.3	0.24	0.80
1H-3, 50–52	3.5	0.28	0.58
1H-3, 70–72	3.7	0.48	0.67
1H-3, 100–102	4	0.68	0.71
1H-3, 120–122	4.2	0.65	0.72
1H-3, 140–142	4.4	0.53	0.93
1H-4, 10–12	4.6	0.21	1.09
1H-4, 30–32	4.8	0.15	0.94
1H-4, 50–52	5	0.19	1.10
1H-4, 66–68	5.16	–0.22	1.27
1H-CC, 20–22	5.42	–0.04	0.92
2H-1, 20–22	5.6	0.92	1.34
2H-1, 42–44	5.82	0.48	1.23
2H-1, 62–64	6.02	0.40	1.31
2H-1, 80–82	6.2	0.54	1.22
2H-1, 100–102	6.4	0.63	1.09
2H-1, 126–128	6.66	0.69	1.02
2H-2, 17–19	7.07	0.41	0.86
2H-2, 30–32	7.2	–0.13	0.53
2H-2, 50–52	7.4	0.02	0.54
2H-2, 70–72	7.6	–0.31	0.47
2H-2, 90–92	7.8	–0.23	0.48
2H-2, 110–112	8	0.31	0.33
2H-2, 132–134	8.22	0.36	0.36
2H-4, 76–78	9.78	0.33	0.37
2H-CC, 14–16	9.96	–0.04	0.36
3H-1, 40–42	10.4	0.19	0.53
3H-1, 60–62	10.6	0.22	0.60
3H-1, 78–80	10.78	–0.05	0.50
3H-2, 50–52	11.32	0.19	0.91
3H-2, 68–70	11.5	–0.04	0.64
3H-CC, 0–2	11.56	–0.22	0.81
4H-2, 76–78	13.86	0.17	0.38
4H-2, 101–103	14.11	–0.33	0.50
4H-2, 126–128	14.36	–0.18	0.35
4H-2, 144–146	14.54	–0.09	0.31
4H-3, 4–6	14.64	–0.52	0.47
4H-3, 26–28	14.86	–0.01	0.38
4H-3, 50–52	15.1	–0.05	0.30
4H-3, 74–76	15.34	0.26	0.35
4H-3, 136–138	15.96	0.53	0.18
4H-4, 22–24	16.32	0.51	0.59
4H-4, 40–42	16.5	0.24	0.28
4H-4, 61–63	16.71	0.31	0.30
4H-5, 45–47	17.56	–0.01	0.44
4H-5, 62–64	17.73	–0.18	0.74
4H-6, 4–6	17.88	–0.03	0.40
4H-6, 22–24	18.06	0.06	0.30
4H-6, 47–49	18.31	–0.29	0.63
4H-6, 78–80	18.62	0.16	0.38
4H-CC, 0–2	18.65	–0.15	0.41
5H-1, 92–94	19.72	–0.40	0.49
5H-1, 148–150	20.28	–0.36	0.52
5H-2, 10–12	20.4	–0.40	0.50
5H-2, 30–32	20.6	–0.08	0.26
5H-2, 66–68	20.96	0.40	0.09
5H-2, 88–90	21.18	0.98	–0.09
5H-2, 110–112	21.4	0.59	–0.11
5H-2, 130–132	21.6	0.77	0.11
5H-2, 148–150	21.78	1.08	–0.07
5H-3, 10–12	21.9	1.13	0.23
5H-3, 30–32	22.1	0.91	0.11
5H-4, 16–18	22.46	0.57	0.08
5H-4, 54–56	22.95	0.41	–0.02
5H-4, 66–68	23.15	0.55	0.31
5H-4, 80–82	23.41	0.34	0.06
5H-4, 104–106	23.65	0.73	–0.01
5H-cc, 0–2	23.72	–0.16	0.35
6H-1, 10–12	24.2	–0.48	0.42
6H-1, 130–132	25.1	–0.21	0.46
6H-2, 50–52	25.8	–0.11	0.79
6H-2, 70–72	26	–0.65	0.27
6H-2, 110–112	26.4	–0.70	0.46
6H-3, 30–32	27.1	0.17	0.65
6H-3, 115–117	27.95	0.18	0.82
6H-4, 10–12	28.4	–0.20	0.88
6H-4, 30–32	28.6	–0.31	0.92
6H-4, 50–52	28.8	–0.26	0.75
6H-4, 70–72	29	0.27	0.74
6H-4, 122–124	29.52	–0.09	0.93
6H-4, 148–150	29.78	0.03	1.07
6H-5, 75–77	30.55	0.09	0.81
6H-5, 94–96	30.74	0.14	0.49
6H-5, 130–132	31.1	1.16	0.09
6H-7, 30–32	32.61	0.96	0.66
7H-1, 60–62	33.9	–0.28	1.15
7H-1, 90–92	34.2	–0.03	1.34
7H-1, 110–112	34.4	0.49	1.37
7H-1, 140–142	34.7	0.45	1.35
7H-2, 12–14	34.92	–0.00	1.11
7H-2, 32–34	35.12	0.61	1.35
7H-2, 54–56	35.34	0.17	0.94
7H-2, 78–80	35.52	0.48	1.17
7H-2, 102–104	35.82	0.06	1.09
7H-2, 130–136	36.1	0.38	1.18
7H-3, 12–14	36.42	0.41	1.19
7H-3, 38–40	36.68	–0.11	0.99
7H-3, 64–66	36.94	0.14	1.07
7H-3, 110–112	37.4	0.38	1.20
7H-4, 14–16	37.94	0.31	1.15
7H-4, 34–36	38.14	0.30	1.11
7H-4, 56–58	38.36	0.63	1.19
7H-4, 116–118	38.96	0.59	1.29
8F-1, 80–82	39.9	0.41	1.09
8F-1, 116–118	40.26	0.63	0.86
8F-CC, 0–2	40.57	–0.02	0.59
9F-2, 74–76	42.84	0.66	0.63
9F-2, 100–102	43.1	0.42	0.21
10F-2, 22–24	46.42	1.10	0.25
10F-2, 46–48	46.66	1.01	0.28
10F-2, 72–74	46.92	0.65	0.14
10F-3, 64–66	48.34	0.28	0.53
10F-3, 90–92	48.6	0.25	0.43
10F-3, 112–114	48.82	0.07	0.41
11F-1, 68–70	49.88	0.12	0.37
11F-2, 54–56	50.95	0.19	0.42
11F-2, 78–80	51.19	0.23	0.80
11F-2, 104–106	51.45	0.31	0.36
11F-2, 130–132	51.71	0.54	–0.04
11F-CC, 7–9	51.83	0.04	0.16
12F-1, 90–92	52.8	0.19	0.49
13F-1, 130–132	53.2	0.79	0.21
13F-CC, 0–2	56.64	0.03	0.62
14F-1, 50–52	57.2	–0.09	0.25
14F-1, 76–78	57.46	–0.06	0.28
14F-1, 104–106	57.74	–0.12	0.18
14F-1, 130–132	58	–0.05	0.27
14F-2, 0–2	58.2	–0.02	0.55
14F-2, 52–54	58.72	–0.02	0.15
14F-2, 90–92	59.1	–0.25	0.34
14F-CC, 16–18	59.47	–0.12	0.24
15F-1, 90–92	60.4	0.09	0.15

Table T1 (continued).

Core, section, interval (cm)	Top depth CSF-A (m)	$\delta^{18}O$ (‰ VPDB)	$\delta^{13}C$ (‰ VPDB)	Core, section, interval (cm)	Top depth CSF-A (m)	$\delta^{18}O$ (‰ VPDB)	$\delta^{13}C$ (‰ VPDB)	Core, section, interval (cm)	Top depth CSF-A (m)	$\delta^{18}O$ (‰ VPDB)	$\delta^{13}C$ (‰ VPDB)
15F-2, 20–22	60.64	–0.51	0.28	16F-CC, 23–25	64.71	0.61	0.11	17F-2, 70–72	66.9	0.24	0.26
15F-2, 80–82	61.24	–0.37	0.31	17F-1, 58–60	65.28	0.60	0.40	17F-2, 96–98	67.16	0.20	–0.23
15F-CC, 0–2	61.26	–0.12	0.11	17F-1, 70–72	65.4	0.25	0.06	17F-CC, 0–2	67.31	0.41	–0.07
16F-1, 120–122	62.5	–0.12	0.24	17F-1, 102–104	65.72	0.28	0.02	18F-2, 80–82	69.7	0.31	–0.07
16F-2, 66–68	63.46	0.67	–0.10	17F-1, 128–130	65.98	0.21	–0.01	18F-CC, 16–18	70.29	0.52	0.04
16F-3, 10–12	63.81	0.67	–0.01	17F-2, 12–14	66.32	0.33	0.15				
16F-3, 28–30	63.99	0.76	0.04	17F-2, 40–42	66.6	0.18	–0.25				

Table T2. Tie points, Hole U1436C. **Download table in .csv format.**

Top depth CSF-A (m)	LR04 age (ka)	Corresponding marine isotope stage
0.00	0.00	
0.71	8.96	MIS 1–MIS 2 transition
1.68	18.12	MIS 2
2.19	36.03	
3.11	54.85	
4.02	62.26	
5.45	85.36	
6.64	108.48	
7.78	131.86	MIS 6–MIS 5 transition
9.78	165.14	
11.44	219.47	
14.64	239.16	MIS 7e
17.73	282.68	
18.06	294.48	
18.62	300.14	
20.03	325.84	
21.78	341.00	MIS 10
23.72	393.04	
24.20	400.96	MIS 11–MIS 10 transition
26.51	411.01	
31.18	434.19	MIS 12
33.85	490.38	MIS 13
34.20	506.42	
35.13	536.12	
35.80	562.03	
36.70	575.44	MIS 15
40.61	610.92	
46.38	629.97	MIS 16
46.91	655.73	
48.82	689.68	MIS 17
51.71	745.83	
51.85	775.68	
52.30	779.42	
53.38	784.95	MIS 20
55.45	795.13	
56.62	817.11	
60.72	858.07	MIS 21
63.99	875.49	MIS 22
66.66	910.40	
70.33	919.73	MIS 24

Figure F4. A. Sedimentation rate curve (depth vs. age) between tie points (see Table **T2**) used in the correlation between LR04 (Lisiecki and Raymo 2005) reference series and Hole U1436C $\delta^{18}O$ curve (produced using AnalySeries 2.0.4.2 software). Age model shows two extreme sedimentation rate intervals: X (red) = very low rate (~0.4 cm/ky; maximum) at the end of MIS 19 (i.e., quasi-hiatus), Y (blue) = very high rate (~400 cm/ky) during MIS 11. Green line = average slope for entire section (~7.5 cm/ky), horizontal red line = black glass mafic ash layer. B. Sedimentary description (shown wrapped in A). Orange = all ash beds but the 10 thinnest, green = layers with coring disturbances (see the **Expedition 350 summary** chapter [Tamura et al., 2015b]).

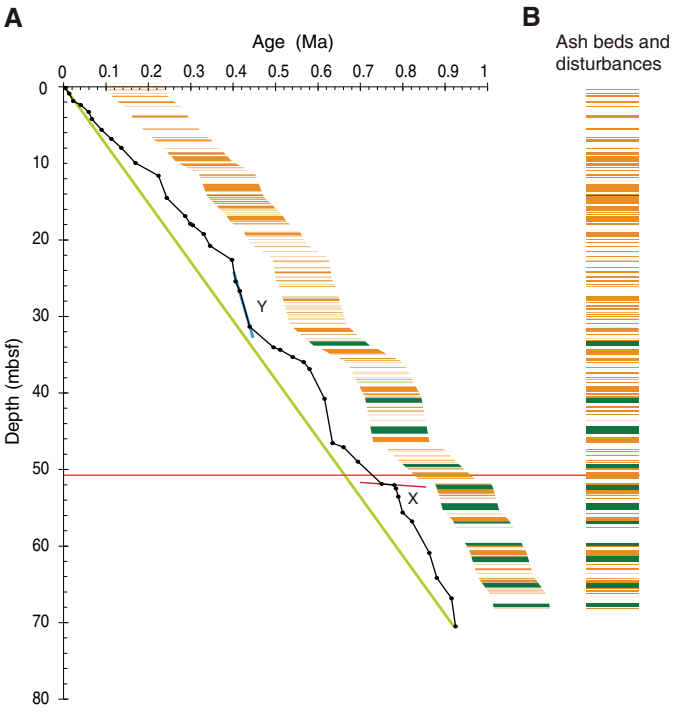

Results

As already noted, the lack of a suitable amount of carbonate in some samples was caused by a combination of biogenic particle dilution by volcaniclastics, which is attested by the numerous volcaniclastic beds observed at this site (Figure **F4B**), and by the absence of well-preserved carbonate in some intervals (e.g., Sample 350-U1436C-10F-2, 72–74 cm [46.92 mbsf], and between Samples 6H-1, 50–52 cm, and 6H-2, 10–12 cm [between 22.92 and 25.4 mbsf]).

Interpretation about the significance of carbonate dissolution intervals will be presented elsewhere in conjunction with other micropaleontological data (Vautravers et al., submitted). However, outside of these intervals, satisfactory values of $\delta^{18}O$ and $\delta^{13}C$ were obtained and provide, as expected, a fairly continuous record (on average three analyses per 1.5 m long section) throughout the entire stratigraphic sequence recovered in Hole U1436C. Although numerous ash layers can be recognized at Site U1436, the conspicuous black glassy mafic ash layer first noted in Hole U1436A is sufficiently distinctive to be confidently identified in Hole U1436C, where it was sampled from interval 11F-1, 106 cm, through 11F-2, 40 cm (from 50.26 to 50.81 mbsf), and is marked on Figures **F2**, **F3**,

and **F4** for an additional visual reference. A precise age modeling exercise was therefore envisaged with confidence and is described below.

A plot of $\delta^{18}O$ and $\delta^{13}C$ versus depth (Figure **F2**) shows the cyclic oxygen and carbon isotopic fluctuations between –0.7‰ (Sample 350-U1436C-6H-2, 110 cm; 26.4 mbsf) and 1.16‰ (6H-5, 130 cm; 31.1 mbsf) for $\delta^{18}O$ and –0.25‰ (17F-2, 40 cm; 66.6 mbsf) and 1.37‰ (7H-1, 110 cm; 34.4 mbsf) for $\delta^{13}C$.

The age model is established using a standard visual correlation method between the newly produced $\delta^{18}O$ data (Figures **F2**, **F3C**) and the $\delta^{18}O$ benthic stack record (LR04) of Lisiecki and Raymo (2005) (Figure **F3B**) and by selecting 40 tie points at notable places on the record (see Table **T2** for a full list). The $\delta^{18}O$ record from Hole U1436C was then transferred into an age scale between each of the selected ties points using the AnalySeries 2.0.4.2 software (Paillard et al., 1996). The nannofossil and planktonic foraminifer (PF) datums (see the **Expedition 350 methods** chapter (Tamura et al., 2015a]) for Hole U1436C are shown in Table **T3**, and their depth ranges and averages are also shown on Figure **F3C** and **F3B** (colored boxes and vertical lines), although none were actually used to establish the isotopic stratigraphy proposed here. However, in some cases the position of the datum helped assert choices of possible correlations between the LR04 stack and our data set and confirm the integrity of the record.

Two ancillary outcomes arise from conducting this comparison exercise. The first outcome shows that the biostratigraphy (based on datums) is much less precise than the stable isotope stratigraphy. In Hole U1436C, this may result from the relatively low sedimentation rate (only ~7.5 cm/ky for the entire Hole U1436C section) coupled with the very low resolution of the shipboard biostratigraphy, (i.e., based on only one observation every 5–9 m). The second outcome is that the bottom occurrences (i.e., first occurrences) of planktonic foraminifers (PF B) (yellow on Figure **F3**) seem to be unreliable. These datums do not fit with the proposed stratigraphic scheme. The reasons for the latter could be due either to analytical errors during PF determination, which is unlikely to have occurred, or, more likely, to the difficulty of precisely assigning the first occurrence of a relatively rare PF species from sediments that are also rather poor in PF (per gram) because of the pervasive and major dilution by volcaniclastics (see Figure **F4B**) and/or poor carbonate preservation. An additional cause for mismatch comes from possible regional disparities between oceans for some of the datum events used. Indeed, Gradstein et al. (2012) does not present any PF datum for the North Pacific in the studied time interval, nor does it give error bars on the age of the datums for the last 1 My. This systematic mismatch for the three PF B bioevents in the last 1 My and the stable isotope results does not overshadow the overall good agreement. This is especially true if the challenges in hand for a site so proximal to a major submarine volcanic caldera are considered. Therefore, Hole U1436C seems, as predicted by the shipboard biostratigraphy (see the **Site U1436** chapter [Tamura et al., 2015c]), to record a rather complete section of Pleistocene paleoceanography and paleoclimatology, interrupted by quasi-instantaneous volcanic depositional events that are traced by ash and lapilli layers in the sequence and for which a detailed study of history is needed, but for which also a solid stratigraphic framework will clearly be an asset.

The representation of the changing sedimentation rates between the 40 selected tie points used to establish the stratigraphy is given on Figure **F4A**. The average sedimentation rate over the last 910 ky (green slope on figure) is ~7.5 cm/ky. However, unsurprisingly and obviously apparent on this figure is the extreme variable nature of these sedimentation rates (SR) (four orders of magnitude). In these volcaniclastics, the sedimentation rates are between two extreme values: (1) 0.4 cm/ky (estimate), for example, during an interval labeled X (red slope on figure) and centered at ~760 ka (late MIS 19) and (2) another value at almost 400 cm/ky (estimate) for an interval labeled Y (blue slope on figure) and centered at ~420 ka (early MIS 11). Several other high-SR intervals are recorded, in particular one at the MIS 16–MIS 15 transition (619–610 ka). The first value corresponds effectively to an apparent hiatus in the record. A hiatus was already inferred by biostratigraphic results within this age range at a similar stratigraphic position relative to the black glassy ash layer also recovered during Leg 126 at Site 792 (Shipboard Scientific Party, 1990). In addition, examination of the sedimentary composition (Figure **F4B**) also shows that Hole U1436C includes many volcaniclastic beds as well as significant sedimentary disturbances, the latter being more abundant toward the base of the section, especially below the break in sedimentation discussed above (X on Figure **F4A**). Therefore, in the context of a mismatch with a single datum (~0.750 Ma) as explained above and what seems to be an important volcaniclastic layer (black glassy mafic ash) found above it at about 0.7 Ma, one must remain cautious. MIS 17 could be incomplete and/or MIS 16 could be resting directly on MIS 19. If this was the case, perhaps a major eruption that would have emplaced the black glassy ash layer could have been responsible for a relatively short hiatus that the stable isotopes may not be able to clearly detect but that seems clear in the low sedimentation rate recorded within this interval. The uncertainty remains until paleo-

Table T3. Microfossil datums, ages, and depths, Hole U1436C. * = datum range fits with isotopic stratigraphy. T = top, B = bottom, Tc = top common occurrence, X = crossover. **Download table in .csv format.**

	Datum	Age (Ma)	Top core, section	Top depth (mbsf)	Bottom core, section	Bottom depth (mbsf)	Average depth (mbsf)	± (m)
			350-U1436C-		350-U1436C-			
Nannofossil	X *Gephyrocapsa caribbeanica–Emiliania huxleyi**	0.09	1H-CC	5.42	2H-CC	10.01	7.74	2.27
	B *Emiliania huxleyi**	0.29	3H-CC	11.56	4H-CC	18.65	15.10	3.55
	T *Pseudoemiliania lacunosa**	0.44	5H-CC	23.77	6H-CC	33.24	28.50	4.74
	Tc *Reticulofenestra asanoi**	0.91	16F-CC	64.76	17F-CC	67.38	66.07	1.31
Planktonic foraminifer	T *Globigerinoides ruber* (pink)*	0.12	1H-CC	5.47	2H-CC	10.01	7.74	2.27
	B *Globigerinella calida*	0.22	1H-CC	5.42	2H-CC	9.96	7.69	2.27
	B *Globigerinoides ruber* (pink)	0.4	6H-CC	33.19	7H-CC	39.02	36.40	2.92
	T *Globorotalia tosaensis**	0.61	7H-CC	39.07	8F-CC	40.62	39.85	0.75
	B *Globorotalia hessi*	0.75	9F-CC	44.67	10F-CC	49.22	46.95	2.28

magnetic measurements on samples from Hole U1436C confirm the position of the Brunhes/Matuyama reversal (aged 0.781 Ma) in depth (at the moment Figure **F3C** only provides an estimate of this position based on the current study) and/or an absolute date for the black glassy ash layer is obtained. Additional information about the nature of this layer could also come from increasing the time resolution in this part of the section with tools similar to those presented here (i.e., stable isotopes and foraminiferal content). In all cases, it is important to keep in mind that Figure **F3** represents only one interpretation, and further studies of sediments from Hole U1436C will bring modifications to the age model suggested by our study. Also, the extremely high sedimentation rates in the time interval Y corresponding to early MIS 11 will need further investigation to understand better what caused them (e.g., sedimentary style involved). Already, Figure **F4B** points to a large number of volcaniclastic beds in this part of the section.

The minimal $\delta^{18}O$ value found at 26.4 mbsf for one sample (350-U1436C-6H-2, 110 cm) representing the early part of the major interglacial MIS 11 (Figure **F3A**) corresponds to an age of 410 ka. Such a light value denotes a composite record of strong warming in the western Pacific Ocean, low global ice volume, and potentially fresher local thermocline water in the vicinity of the Kuroshio Current. Similarly, light values are only found for interglacial MIS 21 (~855 ka) and MIS 7 (~235 ka). In contrast, the maximum value of 1.16‰ for Sample 6H-5, 130 cm, is indicative of a mixed signal between a very large ice volume and a very cold western Pacific Ocean and occurred at ~433 ka during MIS 12. Other approaching heavy values are also found during MIS 16 (~630 ka) and MIS 10 (~342 ka), two major glacial stages known during the Upper Pleistocene.

The $\delta^{13}C$ versus depth plot also shows some meaningful fluctuations. The maximum value is found for one sample (350-U1436C-7H-1, 110 cm; 34.4 mbsf) corresponding to MIS 13 (~490 ka), and similar heavy values, denoting major changes in the global carbon cycle coupled with changes in the global ocean circulation, are found in the later stages of some interglacials such as MIS 5 (i.e., the previous interglacial, ~120 ka) and during MIS 3 (~50 ka, during the previous glacial sensu lato). Also, in general, rather than showing clear cyclicity, $\delta^{13}C$ shows two styles of values: one rather light style (<0.8‰) before MIS 15 (from ~610 to 920 ka) and during an interval corresponding to the time span from MIS 6 to MIS 10 (130–380 ka), and another style occurring during two intervals with values >0.8‰, during MIS 14 and MIS 13 as well as MIS 11, MIS 5, and MIS 3. This observation is puzzling because it tends to suggest that in the western tropical North Pacific near the Kuroshio Current there could be decoupling between the record of the carbon cycle/ocean circulation on one side and temperature/ice volume on the other side. This observation, despite clearly falling outside the scope of this data report, may be worth further investigation.

In summary, this data report on the isotopic analyses clearly demonstrates the existence of climatic cycles at Site U1436. It also shows that their expected relative amplitudes are preserved in the record at this site in most cases (e.g., very strong glacials MIS 16 and MIS 12). Also shown in the figures is the remarkable amplitude of interglacial MIS 11 as well as the hint of a potential very intense carbonate dissolution event at 1776 m water depth, which in this sample set appears like a barren interval during the later part of MIS 11. Remarkably, the stratigraphic position of the black glassy mafic ash layer, which perhaps traces a major and yet unknown volcanic eruption that could have originated in the Izu arc and initially caught the attention of the Expedition 350 scientists in Hole U1436A, falls during MIS 17. That is just before MIS 16 and the onset of the first very strong glacial at the end of the mid-Pleistocene revolution. This was a time that saw major changes in Earth's climate and ocean circulation, primarily involving the intensification of glacial stages and the development of climatic cycles paced by the 100 ky orbital eccentricity cycle, in contrast to 41 ky cycles prior to this interval (Hodell et al., 2008).

Despite a yet rather imprecisely resolved stratigraphy within the time range of interest, between 650 and 750 ka (datum mismatch, black glassy mafic ash layer above an interval of quasi-hiatus in sedimentation), and in view of the extremely contentious role attributed to volcanism on long-term paleoclimatic changes or in reverse of paleoclimatic changes on volcanic eruptions (e.g., via sea level), it seems difficult to call for any potential causal link in this instance. Nonetheless, the distinctive nature of the black glassy mafic ash layer, its potentially large size (perhaps linked to a large-amplitude explosive eruption), and its potentially remarkable stratigraphy together with the large number of volcaniclastic beds now framed by a "classical" oxygen stable isotopic stratigraphy, should undoubtedly justify that Hole U1436C deserves to be studied in greater detail in the future.

Acknowledgments

This research used samples and data provided by the International Ocean Discovery Program (IODP). We acknowledge IODP Expedition 350 Co-Chief Scientists Cathy Busby and Yoshi Tamura, Staff Scientist Peter Blum, shipboard scientists, technical staff, and the crew of the *JOIDES Resolution* as well as the technical staff of IODP Expedition 351, who took samples during transit to help my prompt study. We are grateful to Rob Musgrave for checking and editing the draft version of this manuscript and to Martin Jutzeler for helping with the production of Figure **F4**. Helpful comments from the external reviewer are gratefully acknowledged. Oxygen isotopic measurements were performed in the Godwin Laboratory for Paleoclimatic Research. Thanks are due to James Rolf for supervising the isotopic and sediment preparation facilities in the Earth Sciences Department (Cambridge University) and to Ian Mather for operating the mass spectrometer (Gasbench) in the Godwin Laboratory. Funding for this research was provided by NERC via a post-cruise grant UK-IODP grant number RG 74950 to Maryline Vautravers. Thanks are due to David Hodell for administrating the project and allowing access to the laboratories.

References

Emiliani, C., 1955. Pleistocene temperatures. *The Journal of Geology,* 63(6):538–578. **http://dx.doi.org/10.1086/626295**

Gradstein, F.M., Ogg, J.G., Schmitz, M.D., and Ogg, G.M. (Eds.), 2012. *The Geological Time Scale 2012:* Oxford, United Kingdom (Elsevier).

Hodell, D.A., Channell, J.E.T, Curtis, J.H., Romero, O.E., and Rohl, U., 2008. Onset of "Hudson Strait" Heinrich events in the eastern North Atlantic at the end of the middle Pleistocene transition (~640 ka)? *Paleoceanography,* 23(4):PA4218. **http://dx.doi.org/10.1029/2008PA001591**

Lisiecki, L.E., and Raymo, M.E., 2005. A Pliocene–Pleistocene stack of 57 globally distributed benthic $\delta^{18}O$ records. *Paleoceanography,* 20(1):PA1003. **http://dx.doi.org/10.1029/2004PA001071**

Paillard, D., Labeyrie, L., and Yiou, P., 1996. Macintosh program performs time-series analysis. *Eos, Transactions of the American Geophysical Union,* 77(39):379. **http://dx.doi.org/10.1029/96EO00259**

Shackleton, N., 1967. Oxygen isotope analyses and Pleistocene temperatures re-assessed. *Nature,* 215(5096):15–17. **http://dx.doi.org/10.1038/215015a0**

Shipboard Scientific Party, 1990. Site 792. *In* Taylor, B., Fujioka, K., et al., *Proceedings of the Ocean Drilling Program, Initial Reports,* 126: College Station, TX (Ocean Drilling Program), 221–314. **http://dx.doi.org/10.2973/odp.proc.ir.126.109.1990**

Tamura, Y., Busby, C.J., Blum, P., Guèrin, G., Andrews, G.D.M., Barker, A.K., Berger, J.L.R., Bongiolo, E.M., Bordiga, M., DeBari, S.M., Gill, J.B., Hamelin, C., Jia, J., John, E.H., Jonas, A.-S., Jutzeler, M., Kars, M.A.C., Kita, Z.A., Konrad, K., Mahony, S.H., Martini, M., Miyazaki, T., Musgrave, R.J., Nascimento, D.B., Nichols, A.R.L., Ribeiro, J.M., Sato, T., Schindlbeck, J.C., Schmitt, A.K., Straub, S.M., Vautravers, M.J., and Yang, Y., 2015a. Expedition 350 methods. *In* Tamura, Y., Busby, C.J., Blum, P., and the Expedition 350 Scientists, *Izu-Bonin-Mariana Rear Arc.* Proceedings of the International Ocean Discovery Program, 350: College Station, TX (International Ocean Discovery Program). **http://dx.doi.org/10.14379/iodp.proc.350.102.2015**

Tamura, Y., Busby, C.J., Blum, P., Guèrin, G., Andrews, G.D.M., Barker, A.K., Berger, J.L.R., Bongiolo, E.M., Bordiga, M., DeBari, S.M., Gill, J.B., Hamelin, C., Jia, J., John, E.H., Jonas, A.-S., Jutzeler, M., Kars, M.A.C., Kita, Z.A., Konrad, K., Mahony, S.H., Martini, M., Miyazaki, T., Musgrave, R.J., Nascimento, D.B., Nichols, A.R.L., Ribeiro, J.M., Sato, T., Schindlbeck, J.C., Schmitt, A.K., Straub, S.M., Vautravers, M.J., and Yang, Y., 2015b. Expedition 350 summary. *In* Tamura, Y., Busby, C.J., Blum, P., and the Expedition 350 Scientists, *Izu-Bonin-Mariana Rear Arc.* Proceedings of the International Ocean Discovery Program, 350: College Station, TX (International Ocean Discovery Program). **http://dx.doi.org/10.14379/iodp.proc.350.101.2015**

Tamura, Y., Busby, C.J., Blum, P., Guèrin, G., Andrews, G.D.M., Barker, A.K., Berger, J.L.R., Bongiolo, E.M., Bordiga, M., DeBari, S.M., Gill, J.B., Hamelin, C., Jia, J., John, E.H., Jonas, A.-S., Jutzeler, M., Kars, M.A.C., Kita, Z.A., Konrad, K., Mahony, S.H., Martini, M., Miyazaki, T., Musgrave, R.J., Nascimento, D.B., Nichols, A.R.L., Ribeiro, J.M., Sato, T., Schindlbeck, J.C., Schmitt, A.K., Straub, S.M., Vautravers, M.J., and Yang, Y., 2015c. Site U1436. *In* Tamura, Y., Busby, C.J., Blum, P., and the Expedition 350 Scientists, *Izu-Bonin-Mariana Rear Arc.* Proceedings of the International Ocean Discovery Program, 350: College Station, TX (International Ocean Discovery Program). **http://dx.doi.org/10.14379/iodp.proc.350.103.2015**

Vautravers, M.J., and Expedition 350 Scientists, submitted. Quantitative foraminifer taphonomy and paleoceanographic implications at intermediate water depth in the subtropical western North Pacific over the last 1 My from IODP Expedition 350 Sites U1436 and U1437, Izu arc area. *Marine Micropaleontology*.

Vautravers, M.J., Hodell, D.A., Channell, J.E.T., Hillenbrand, C.-D., Hall, M., Smith, J., and Larter, R.D., 2013. Palaeoenvironmental records from the West Antarctic Peninsula drift sediments over the last 75 ka. *In* Hambrey, M.J., Barker, P.F., Barrett, P.J., Bowman, V., Davies, B., Smellie, J.L., and Tranger, M. (Eds.), *Antarctic Palaeoenvironments and Earth-Surface Processes.* Geological Society Special Publication, 381:263–276. **http://dx.doi.org/10.1144/SP381.12**

Vautravers, M.J., Shackleton, N.J., Lopez-Martinez, C., and Grimalt, J.O., 2004. Gulf Stream variability during marine isotope Stage 3. *Paleoceanography,* 19(2):PA2011. **http://dx.doi.org/10.1029/2003PA000966**